Journal of Solid State Chemistry 183 (2010) 2835–2844

Contents lists available at ScienceDirect

Journal of Solid State Chemistry

journal homepage: www.elsevier.com/locate/jssc

A new polymorph of $Ba(AsO_3OH)$: Synthesis, crystal structure and vibrational spectra

Tamara Đorđević [a,*], Ljiljana Karanović [b]

[a] Institut für Mineralogie und Kristallographie, Geozentrum, Universität Wien, Althanstrasse 14, A-1090 Wien, Austria
[b] Laboratory of Crystallography, Faculty of Mining and Geology, Đušina 7, 11000 Belgrade, Serbia

ARTICLE INFO

Article history:
Received 28 June 2010
Received in revised form
2 September 2010
Accepted 19 September 2010
Available online 25 September 2010

Keywords:
$Ba(AsO_3OH)$
Hydrothermal synthesis
Single crystal structure analysis
Raman spectroscopy
Infrared spectroscopy
Hydrogen bonds
Alkaline earth hydrogen arsenates

ABSTRACT

A new monoclinic polymorph of $Ba(AsO_3OH)$ was synthesized under hydrothermal conditions. It represents a previously unknown structure type. Its crystal structure was determined from a racemic twin using single-crystal X-ray diffraction data collected at 120 and 293 K [space group $P2_1$, $a=7.2149(14)/7.2370(2)$, $b=7.7028(15)/7.7133(2)$, $c=21.7385(43)/21.8079(5)$ Å, $\beta=95.95(3)/96.073(1)^\circ$, $V=1201.6(4)/1210.51(5)$ Å^3, $Z=12$]. The crystal structure of $P2_1$-$Ba(AsO_3OH)$ has a layered character and is built up of four types of regularly alternating layers parallel to (0 0 1). Every AsO_3OH tetrahedron is chelating to two Ba atoms and bridged by another two Ba atoms. Each OH group acts as hydrogen bond donor toward the oxygen atoms positioned in the same or adjacent layers. Although the H atoms could not be located, no ambiguities are present in the hydrogen-bonding scheme. Single-crystal vibrational spectroscopy (FTIR and Raman) was used to describe the vibrational behavior of the hydrogen bond system; particularly the spectroscopic manifestation of the very short and short hydrogen bonds (2.462(7)–2.575(7) Å). In order to complement spectroscopic data on protonated orthoarsenates, infrared spectra of triclinic $F\bar{1}$-$Sr(AsO_3OH)$ and the orthorhombic variety of *Pbca*-$Ba(AsO_3OH)$ were recorded and discussed. Furthermore, structural features of other alkaline earth hydrogen arsenates are discussed.

1. Introduction

The chemistry of hydrated and anhydrous barium hydrogen arsenates has been well known for a long time [1–4 and references therein]. However, not much is known about their structural features. The synthesis and structural characterization of compounds in the BaO—As_2O_5—H_2O system revealed only a small number of compounds so far. Guerin [2] found three stable compounds at 30 °C: $BaHAsO_4\cdot H_2O$, $BaH_4(AsO_4)_2\cdot H_2O$ and $3As_2O_5\cdot 5H_2O$. Martin et al. [5] determined the crystal structure of $BaHAsO_4\cdot H_2O$ from a crystal obtained by hydrolysis of $Ba_2As_2O_7$. Blum et al. [6] reported the crystal structure of orthorhombic $BaH_6As_4O_{14}$, which contains a new type of cyclic As_4O_{14} anion, involving AsO_4 tetrahedra and AsO_6 octahedra. Nabar & Dalvi [7] isolated both $BaHAsO_4$ and $Ba_2As_2O_7$ as heating products of $BaHAsO_4\cdot H_2O$. According to the published X-ray powder diffraction data this $BaHAsO_4$ should be isostructural with orthorhombic *Pbnm*-$BaHPO_4$ [8,9]. A second, also orthorhombic form of *Pbca*-$Ba(AsO_3OH)$ isotypic with γ-$SrHPO_4$ [10] was reported in Ref. [11].

An ongoing study concerning the hydrothermal synthesis, crystallography and properties of arsenate and vanadate(V) compounds in the system $M1O$–$M2O$–X_2O_5–H_2O ($M1=Sr^{2+}$, Cd^{2+}, Ba^{2+}, Bi^{3+}, Hg^{2+}; $M2=Mg^{2+}$, $Mn^{2+,3+}$, $Fe^{2+,3+}$, Co^{2+}, Ni^{2+}, Cu^{2+}, Zn^{2+}; $X=As^{5+}$, V^{5+}) yielded a large number of new $M1^{2+}$–(H–)-, $M2^{2+}$–(H–)- and $M1$–$M2$–(H–) arsenates and vanadates [11–16] that were characterized structurally, and, in part, also by spectroscopic techniques. Among them, a new polymorph of $P2_1$-$Ba(AsO_3OH)$ has been obtained, which also represents a new structure type. Here are reported its hydrothermal synthesis and crystal structure. Furthermore, single-crystal Raman and infrared spectra were acquired to obtain further information on both anion groups and especially on the very short hydrogen bond distances, where the donor and acceptor atoms are not equal due to (average) space-group symmetry. In order to compare the spectroscopic data on protonated orthoarsenates, single-crystal infrared spectra of triclinic $F\bar{1}$-$Sr(AsO_3OH)$ [11], and powder infrared and Raman spectra of orthorhombic *Pbca*-$Ba(AsO_3OH)$ [11] have been measured.

In addition, structural similarities to other alkaline earth hydrogen arsenates are discussed. The hydrogen bonds in triclinic, monoclinic and orthorhombic $MHXO_4$ and $M(XO_3OH)$ ($M=Ba^{2+}$, Ca^{2+}, Sr^{2+}; $X=As^{5+}$, P^{5+}) compounds will also be discussed (crystal-chemical formulae are the same as in original papers).

* Corresponding author. Fax: +43 1 4277 9532.
E-mail address: tamara.djordjevic@univie.ac.at (T. Đorđević).

0022-4596/$ - see front matter © 2010 Elsevier Inc. All rights reserved.
doi:10.1016/j.jssc.2010.09.027

2. Experimental

2.1. Hydrothermal synthesis

In course of the experiments aimed at synthesizing compounds with the general formula $M1^{1+,2+}M2^{2+,3+}(OH,O)[X^{4+,5+,6+}(O_4,O_3OH)]$, $M1=Na^+$, Ca^{2+}, Cd^{2+}, Pb^{2+}; $M2=Mg^{2+}$, Al^{3+}, $Mn^{2+,3+}$, Fe^{2+}, Co^{2+}, Ni^{2+}, Cu^{2+}, Zn^{2+}; $X=Si^{4+}$, P^{5+}, V^{5+}, As^{5+}, Mo^{6+} (mineral group descloizite-adelite) using hydrothermal methods, single crystals of $P2_1$-Ba(AsO_3OH) were obtained from a starting mixture of $Ba(OH)_2\cdot 8H_2O$ (Mallinckrodt 3772, > 97%), Zn powder (Riedel-de Haën 14409) and As_2O_5 (Alfa Products 87687, > 99.9%) in a 1:1:1 molar ratio. The mixture was transferred into Teflon vessels and filled to approximately 75% of their volume with distilled water; the pH of the liquid was 2. The vessels were then enclosed into stainless-steel autoclaves and heated under autogeneous pressure from 20 to 220 °C (4 h), held at that temperature (36 h), then cooled to 120 °C (4 h), kept at that temperature (10 h), and finally cooled to room temperature (4 h). At the end of the reaction the pH of the solvent was 5.5, indicating only moderate acidity. Monoclinic $P2_1$-Ba(AsO_3OH) crystallized as colorless, needle-like crystals up to 0.20 mm in length (yield ca. 30%) accompanied with transparent, colorless, prismatic crystals of orthorhombic *Pbca*-Ba(AsO_3OH) (yield ca. 30%) and an uninvestigated white powder (yield ca. 40%). The reaction products were filtered, washed thoroughly with distilled water and dried in air at room temperature. In this hydrothermal reaction Zn was not incorporated in single crystals. In the course of *Pbca*-Ba(AsO_3OH) synthesis reported in Ref. [11] (from the mixture $Ba(OH)_2\cdot 8H_2O+Ni(NO_3)_2\cdot 6H_2O+As_2O_5+H_2O$), Ni was also not incorporated in any of the single crystals. During the synthesis of the orthorhombic polymorph a bit faster cooling rate was used than in this work, which is a possible explanation why only the single crystals of a denser *Pbca*-$BaAsO_3OH$ were formed.

2.2. X-ray diffraction experiments and crystal structure solution

The crystal quality of several single crystals of monoclinic $P2_1$-Ba(AsO_3OH) was checked with a Nonius KappaCCD single-crystal four-circle diffractometer (Mo tube, graphite monochromator, CCD detector frame size: 621 × 576 pixels, binned mode), equipped with a 300 μm diameter capillary-optics collimator. One sample exhibiting sharp reflection spots was chosen for data collection. A complete sphere of reciprocal space (φ and ω scans) was measured at room temperature. In order to find the accurate positions of the H atoms, a low-temperature measurement at 120 K was additionally performed (scan mode: ω scans). This measurement resulted, as expected, in a slightly smaller unit cell. Because the structure refinement of the data collected at 120 K did not reveal significant changes and did not indicate any phase transition, only results found at room temperature study will be used for the crystal-structure description and for illustrations in all figures (see Table 1 and section 3.7 for details). The intensity data were processed with the Nonius program suite DENZO-SMN [17] and corrected for Lorentz, polarization, and background effects and, by the multi-scan method [17,18], for absorption.

The crystal structure was solved by direct methods and refined using standard procedures [19,20]. Anisotropic displacement parameters were allowed to vary for all non-H atoms. Since the six H atoms could not be located, their positions were calculated ($r_{O-H}=0.85$ (2) Å, computer program HYDROGEN [21]) with isotropic atomic displacement parameters approximately 20% larger than those of the corresponding oxygen atom [$U_{iso}(H)=1.2U_{eq}(O)$]. Crystal data, information on the data collection and results of the final structure refinement are compiled in Table 1. The positional and equivalent atomic displacement parameters are given in Table 2, bond distances and bond angles in Table 3. All drawings were produced with ATOMS [22].

Table 1
Crystal data, data collection and refinement details for $P2_1$-Ba(AsO_3OH).

Crystal data		
Chemical formula	$BaAsO_3OH$	$BaAsO_3OH$
Temperature	293(2) K	120(2) K
Formula weight, M_r (g/mol)	277.27	277.27
Space group (No.), Z	$P2_1$ (4), 12	$P2_1$ (4), 12
a (Å)	7.2370(2)	7.2149(14)
b (Å)	7.7133(2)	7.7028(5)
c (Å)	21.8079(5)	21.739(4)
β (deg.)	96.0730(10)	95.95(3)
V (Å^3)	1210.51(5)	1201.6(4)
Calculated density D_x (g/cm^3)	4.564	4.598
Absorption coefficient, μ (mm^{-1})	17.844	17.977
T_{min}/T_{max}	0.1514/0.6166	0.1501/0.6146
Crystal size (mm^3)	0.17 × 0.07 × 0.03	0.17 × 0.07 × 0.03
Data collection		
Crystal-detector distance (mm)	38	38
Rotation width (deg.)	2	2
Total no. of frames	621	462
Collection time per frame (s)	100	150
Absorption correction	Multi-scan	Multi-scan
Reflections collected/unique	10355/5800	5946/5946
Observed reflections [$I>2\sigma(I)$]	5661	5655
R_{int}	0.0261	0.0323
θ_{max} (deg.)	32.577	34.95
Refinement		
Extinction coefficient, k [a]	0.00088(7)	0.00033(7)
Refined parameters	327	327
Number of restraints	1	1
R-indices [$I>2\sigma(I)$]	$R_1=0.0242$ $wR_2=0.0671$	$R_1=0.0325$ $wR_2=0.0828$
R-indices (all data)	$R_1=0.0252$ $wR_2=0.0676$	$R_1=0.0354$ $wR_2=0.0850$
Flack parameter	0.546(12)	0.535(16)
Goodness-of-fit, S	1.048	1.034
$(\Delta/\sigma)_{max}$	0.002	0.002
$(\Delta\rho)_{max}$, $(\Delta\rho)_{min}$ (e Å^{-3})	1.667, −1.246	1.359, −1.527
a, b [b]	0.0451, 1.2790	0.0588, 2.8650

[a] $F_c^*=kF_c[1+0.001\times F_c^2\lambda^3/\sin(2\theta)]^{-1/4}$.
[b] $w=1/[\sigma^2(F_o^2)+(aP)^2+bP]$.

2.3. Infrared and Raman spectra

Polarized single-crystal infrared spectra of $P2_1$-Ba(AsO_3OH) (size: 0.18 × 0.08 × 0.03 mm^3) were recorded on a Bruker Tensor 27 FTIR spectrophotometer with a mid-IR glowbar light source and KBr beam splitter, attached to a Hyperion 2000 FTIR microscope with liquid nitrogen-cooled mid-IR broad band MCT detector. A total of 128 scans were accumulated between 4000 and 400 cm^{-1} circular sample aperture 100 μm diameter and ATR 15 × objektiv.

For the comparison purposes and in order to compile spectroscopic data for other protonated arsenates, single-crystal FTIR-absorption spectra of triclinic $F\bar{1}$-Sr(AsO_3OH) and powder infrared spectra of orthorhombic *Pbca*-Ba(AsO_3OH) (no big enough single crystals were available) synthesized earlier [11] were recorded with a Perkin Elmer FTIR instrument 1760X at a resolution of 4 cm^{-1}. For powder measurements the sample was prepared as a KBr pellet. A TGS detector was used to collect a total of 128 scans in the range 4000–400 cm^{-1}. Investigations of polarized single-crystal spectra were performed with an attached Perkin Elmer FTIR microscope (circular sample aperture 100 μm diameter, 6 × / 0.60 N.A. mirror lenses (Cassegrains), N_2 cooled wide-range MCT detector, gold-wire grid-polarizer with an extinction ratio better

Table 2
Fractional atomic coordinates and displacement parameters for $P2_1$-Ba(AsO_3OH). U_{equiv} according to [33]. For the H atoms U_{iso} is shown.

	X-ray data at 293 K				X-ray data at 120 K			
Atom	*x*	*y*	*z*	U_{equiv}/U_{iso}	*x*	*y*	*z*	U_{equiv}/U_{iso}
Ba1	0.15278(4)	0.32616(5)	0.997373(16)	0.01133(8)	0.15233(6)	0.32696(7)	0.99751(2)	0.00721(11)
Ba2	0.43881(5)	1.00560(5)	0.831632(19)	0.01309(9)	0.44218(7)	1.00494(6)	0.83107(2)	0.00824(11)
Ba3	−0.26054(5)	0.53430(5)	0.823057(18)	0.01225(9)	−0.26003(7)	0.53339(7)	0.82316(2)	0.00782(11)
Ba4	−0.00008(5)	0.82055(4)	0.685875(17)	0.01064(8)	0.00029(6)	0.82081(6)	0.68568(2)	0.00678(11)
Ba5	0.27890(5)	0.33083(5)	0.669203(17)	0.01132(8)	0.27648(6)	0.33112(7)	0.66915(2)	0.00686(11)
Ba6	0.35833(5)	0.73537(5)	0.518967(18)	0.01098(8)	0.35906(7)	0.73566(6)	0.51908(2)	0.00719(11)
As1	−0.33428(8)	0.34039(9)	0.99154(3)	0.01019(13)	−0.33508(11)	0.34124(13)	0.99185(4)	0.00665(17)
As2	−0.05006(8)	0.99784(8)	0.85474(3)	0.00962(13)	−0.04777(11)	0.99699(11)	0.85445(4)	0.00625(17)
As3	0.24208(8)	0.51274(8)	0.81289(3)	0.00942(13)	0.24155(11)	0.51204(11)	0.81281(4)	0.00632(17)
As4	0.48830(8)	0.83184(9)	0.67811(3)	0.00870(12)	0.48934(11)	0.83162(12)	0.67815(4)	0.00581(16)
As5	−0.22595(8)	0.30574(8)	0.66262(3)	0.00893(13)	−0.22771(11)	0.30694(11)	0.66265(4)	0.00601(18)
As6	−0.15861(8)	0.74264(8)	0.50119(3)	0.00947(13)	−0.15744(11)	0.74259(12)	0.50090(4)	0.00637(17)
O11	−0.2281(6)	0.4888(6)	0.9520(2)	0.0169(10)	−0.2265(8)	0.4894(8)	0.9522(3)	0.0126(13)
O12	0.1856(6)	0.6929(6)	0.9762(2)	0.0137(9)	0.1857(8)	0.6919(8)	0.9759(3)	0.0097(12)
O13	0.4768(6)	0.9211(6)	0.9593(2)	0.0163(10)	0.4781(8)	0.9215(8)	0.9585(3)	0.0112(13)
O14	0.5095(7)	1.2328(6)	0.9386(2)	0.0212(10)	0.5095(8)	1.2346(8)	0.9380(3)	0.0118(12)
H1	0.4890	1.1264	0.9455	0.025	0.5053	1.1264	0.9455	0.014
O21	0.0753(7)	1.0783(7)	0.9161(3)	0.0283(13)	0.0782(9)	1.0785(8)	0.9154(3)	0.0160(14)
O22	0.0787(6)	0.9161(7)	0.8033(2)	0.0209(10)	0.0816(8)	0.9150(8)	0.8029(3)	0.0089(12)
O23	0.7871(6)	0.8633(6)	0.8763(2)	0.0190(10)	0.7874(8)	0.8627(8)	0.8760(3)	0.0103(12)
O24	0.8201(7)	1.1672(6)	0.8159(2)	0.0193(10)	0.8230(9)	1.1675(8)	0.8151(3)	0.0099(12)
H2	0.8438	1.1595	0.7786	0.023	0.8548	1.1595	0.7786	0.012
O31	0.3999(6)	0.6683(6)	0.8237(3)	0.0231(12)	0.4014(8)	0.6685(8)	0.8242(3)	0.0109(13)
O32	0.3486(6)	0.3273(6)	0.8003(2)	0.0211(10)	0.3466(8)	0.3246(8)	0.7996(3)	0.0115(12)
O33	0.0719(6)	0.5413(6)	0.7552(2)	0.0172(10)	0.0699(8)	0.5417(8)	0.7548(3)	0.0105(12)
O34	0.1278(6)	0.5022(6)	0.8791(2)	0.0180(10)	0.1240(8)	0.5018(8)	0.8790(3)	0.0095(12)
H3	0.1428	0.5894	0.9030	0.022	0.1348	0.5891	0.9030	0.011
O41	−0.3368(6)	0.7929(6)	0.7319(2)	0.0172(10)	−0.3358(8)	0.7926(8)	0.7323(3)	0.0118(13)
O42	0.3508(6)	0.6707(6)	0.6497(2)	0.0152(10)	0.3500(8)	0.6693(8)	0.6493(3)	0.0108(13)
O43	0.3536(6)	0.9943(6)	0.6993(2)	0.0173(10)	0.3529(8)	0.9959(8)	0.6986(3)	0.0094(12)
O44	0.5923(7)	0.8963(6)	0.6118(2)	0.0176(10)	0.5957(8)	0.8961(8)	0.6122(3)	0.0092(12)
H4	0.5937	1.0055	0.6067	0.021	0.6014	1.0056	0.6067	0.011
O51	0.6410(6)	0.3830(7)	0.7135(2)	0.0192(10)	0.6387(8)	0.3867(8)	0.7132(3)	0.0120(13)
O52	0.9378(6)	1.1701(6)	0.6933(2)	0.0162(10)	0.9356(8)	1.1706(8)	0.6942(3)	0.0088(12)
O53	0.6338(6)	1.2193(6)	0.6037(2)	0.0138(9)	0.6340(8)	1.2183(8)	0.6035(3)	0.0106(12)
O54	−0.1052(6)	0.4760(6)	0.6308(2)	0.0145(9)	−0.1046(8)	0.4764(8)	0.6302(3)	0.0100(12)
H5	−0.1811	0.5044	0.6000	0.017	−0.1831	0.5039	0.6000	0.012
O61	0.2941(6)	0.3967(6)	0.5322(2)	0.0162(10)	0.2938(8)	0.3973(8)	0.5323(3)	0.0107(13)
O62	−0.0056(6)	0.3177(6)	0.4449(2)	0.0157(9)	−0.0073(8)	0.3173(8)	0.4457(3)	0.0100(12)
O63	−0.2841(6)	0.5781(6)	0.5261(2)	0.0139(9)	−0.2835(8)	0.5764(7)	0.5251(3)	0.0080(11)
O64	−0.0367(7)	0.6593(6)	0.4433(3)	0.0219(11)	−0.0351(9)	0.6590(8)	0.4424(3)	0.0150(14)
H6	−0.0206	0.5504	0.4465	0.026	−0.0206	0.5495	0.4465	0.018

than 100:1 at $< 3500\ cm^{-1}$). A total of 128 scans were accumulated between 4000 and 600 cm^{-1}.

In order to study the arsenate groups in more detail, single-crystal Raman spectra of the both polymorphs of $BaAsO_3OH$ were measured with a Renishaw RM1000 notch filter-based micro-Raman system in the spectroscopic range from 4000 to 60 cm^{-1} for $P2_1$-Ba(AsO_3OH) and from 4000 to 200 cm^{-1} for *Pbca*-Ba(AsO_3OH). The 632.8 nm excitation line of a He–Ne ion laser was used for $P2_1$-Ba(AsO_3OH) and for *Pbca*-Ba(AsO_3OH) the 488.0 nm excitation line of the Ar ion laser was used. The crystals of the both polymorphs were focused with a 50 × /0.75 objective on the crystal faces of the single crystals. Raman intensities were collected with a thermo-electrically cooled CCD array detector. The spectra were acquired with a nominal exposure time of 30 s for $P2_1$-Ba(AsO_3OH) and 120 s for *Pbca*-Ba(AsO_3OH) (resolution: 4–5 cm^{-1}; mode: continuous grating scan mode, 1200 lines/mm grating).

3. Results and discussion

3.1. Description of the crystal structure

The crystal structure of monoclinic $P2_1$-Ba(AsO_3OH) has a layered character and can be divided into four types of regularly alternating layers parallel to (0 0 1) (Fig. 1). These layers host mutually isolated, slightly distorted and differently oriented $AsO_3(OH)$ tetrahedra and Ba atoms between them. There are no significant compositional variations for any of the layers. In the layer I at the margins ($z=0$) and in the layer IV in the central portion of the unit cell ($z=0.5$), Ba1 with $As1O_3OH1$, and Ba6 with $As6O_3OH6$ are situated, respectively. In these two layers the atomic positions of cations are dictated by crystal symmetry, i.e. by presence of screw axes 2_1. Due to the absence of the screw axis 2_1 in each of the middle layers II and III, two crystallographically distinct positions for Ba and As atoms in each layer were found. Within the planes at $z\sim0.167$ and 0.833, Ba2, Ba3, $As2O_3OH2$ and $As3O_3OH3$ polyhedra form layer II. Within the planes at $z\sim0.333$ and 0.667, Ba4 and $As4O_3OH4$ together with Ba5 and $As5O_3OH5$ polyhedra form layer III.

Each layer shares common O atoms and OH groups with adjacent layers. In all four layers AsO_3OH tetrahedra are linked through three O atoms and one OH group to four Ba in the same layer, i.e. every AsO_3OH tetrahedron is chelating to two Ba atoms and bridged by another two Ba atoms. The OH groups act as hydrogen bond donors toward the oxygen atoms positioned in the same or adjacent layers.

The differences in coordination of Ba atoms, which form $BaO_7(OH)_2$ and $BaO_8(OH)_2$ polyhedra, are the consequence of relatively small shifts of oxygen atoms, caused by the different orientation of $AsO_3(OH)$ tetrahedra.

Table 3

Selected bond distances (Å) and bond angles (deg.) for the coordination polyhedra in $P2_1$-Ba(AsO_3OH) (room-temperature data collection). For comparison, average and hydrogen bond lengths for the refinement of the 120 K data are given in *italics*. The variation between room-temperature and low temperature data refinements Δ_T is given in ‰ (in *italics*).

Ba1–O21[a]	2.627(5)	Ba4–O33	2.652(5)	As1–O11	*1.669(5)*
Ba1–O23[b]	2.759(5)	Ba4–O22	2.668(5)	As1–O12[c]	1.669(4)
Ba1–O12[c]	2.772(5)	Ba4–O41	2.740(5)	As1–O13[c]	1.684(5)
Ba1–O13[b]	2.843(4)	Ba4–O52[d]	2.741(5)	As1–O14[e]	1.740(5)
Ba1–O11[c]	2.856(5)	Ba4–O62[f]	2.857(5)	⟨As1[4]–O⟩	1.695
Ba1–O12	2.880(5)	Ba4–O43	2.877(4)		*1.695*
Ba1–O34	2.903(5)	Ba4–O42	2.972(5)	Δ_T	*0‰*
Ba1–O14	3.087(5)	Ba4–O54	2.982(5)		
Ba1–O11	3.094(5)	Ba4–O44[d]	3.262(5)	As2–O21	1.656(5)
Ba1–O21	3.275(6)	⟨Ba4[9]–O⟩	2.862	As2–O22	1.657(5)
⟨Ba1[10]–O⟩	2.910		*2.853*	As2–O23[d]	1.674(5)
	2.903	*ΔT*	*−3.14‰*	As2–O24[d]	1.771(5)
Δ_T	*−2.41‰*			⟨As2[4]–O⟩	1.690
		Ba5–O42	2.715(4)		*1.691*
Ba2–O31	2.621(5)	Ba5–O43[a]	2.718(5)	Δ_T	*+0.59‰*
Ba2–O32[g]	2.638(5)	Ba5–O51	2.725(4)		
Ba2–O22	2.704(5)	Ba5–O32	2.849(5)	As3–O31[h]	1.656(5)
Ba2–O23	2.826(5)	Ba5–O52[e]	2.861(5)	As3–O32[d]	1.661(5)
Ba2–O13	2.844(5)	Ba5–O33	2.999(5)	As3–O33	1.679(5)
Ba2–O43	2.887(5)	Ba5–O54	3.032(4)	As3–O34	1.741(5)
Ba2–O14	2.918(5)	Ba5–O61	3.045(5)	⟨As3[4]–O⟩	1.684
Ba2–O24	3.080(5)	Ba5–O64[i]	3.152(5)		*1.693*
Ba2–O41[h]	3.287(5)	Ba5–O53[a]	3.187(5)	Δ_T	*+5.31‰*
Ba2–O21	3.413(6)	⟨Ba5[10]–O⟩	2.934		
⟨Ba2[10]–O⟩	2.922		*2.916*	As4–O41[h]	*1.660(5)*
	2.910	Δ_T	*−6.13‰*	As4–O42	1.670(4)
Δ_T	*−4.11‰*			As4–O43	1.682(5)
		Ba6–O61	2.674(4)	As4–O44	1.770(5)
Ba3–O31[d]	2.667(5)	Ba6–O53[j]	2.684(5)	⟨As4[4]–O⟩	1.696
Ba3–O51[d]	2.687(5)	Ba6–O44	2.790(5)		*1.700*
Ba3–O23[d]	2.797(5)	Ba6–O62[f]	2.823(4)	Δ_T	*+2.35‰*
Ba3–O11	2.819(5)	Ba6–O63[h]	2.847(4)		
Ba3–O41	2.829(5)	Ba6–O63[f]	2.852(54	As5–O51[d]	1.655(5)
Ba3–O24[e]	2.899(5)	Ba6–O42	2.900(5)	As5–O52[e]	1.667(4)
Ba3–O33	2.954(5)	Ba6–O61[k]	3.117(5)	As5–O53[e]	1.689(4)
Ba3–O34	2.955(5)	Ba6–O64	3.200(5)	As5–O54	1.760(4)
Ba3–O32[d]	3.241(5)	⟨Ba6[9]–O⟩	2.874	⟨As5[4]–O⟩	1.693
⟨Ba3[9]–O⟩	2.872		*2.867*		*1.695*
Δ_T	*2.862*	Δ_T	*−2.44‰*	Δ_T	*+1.16‰*
	−3.48‰				
				As6–O61[f]	1.659(4)
				As6–O62[f]	1.683(4)
				As6–O63	1.684(4)
				As6–O64	1.738(5)
				⟨As6[4]–O⟩	1.691
					1.692
				Δ_T	*+0.59‰*

Hydrogen bonds

Donor (D)	H atom	Acceptor (A)	D–H	H···A	D–H···A	D···A
O14	H1	O13	0.850(5)	1.616(5)	173.1(4)	2.462(7)
			0.850(6)	*1.619(6)*	*175.1(4)*	*2.467(9)* Δ_T*= +2.03‰*
O24	H2	O52	0.850(5)	2.049(5)	170.1(4)	*2.890(7)*
			0.850(6)	*1.984(6)*	*173.3(5)*	*2.830(8)* $\Delta_T = -20.76‰$
O34	H3	O12	0.850(5)	1.783(5)	154.3(4)	*2.575(7)*
			0.849(6)	*1.777(6)*	*153.8(5)*	*2.567(5)* $\Delta_T = -3.11‰$
O44	H4	O53	0.851(5)	1.677(5)	169.8(4)	*2.519(6)*
			0.854(6)	*1.658(6)*	*172.6(4)*	*2.506(9)* $\Delta_T = -5.16‰$
O54	H5	O63	0.850(4)	1.794(5)	164.4(3)	*2.623(6)*
			0.849(6)	*1.800(6)*	*162.0(4)*	*2.621(8)* $\Delta_T = -0.76‰$
O64	H6	O62	0.850(5)	1.798(5)	173.1(4)	*2.644(7)*
			0.853(6)	*1.792(2)*	*172.6(5)*	*2.640(9)* $\Delta_T = -1.51‰$

[a] x, y−1, z.
[b] −x+1, y−1/2, −z+2.
[c] −x, y−1/2, −z+2
[d] x−1, y−1, z
[e] −x, y+1/2, −z+1
[f] x−1, y, z
[g] x, y+1, z
[h] x+1, y, z
[i] −x, y−1/2, −z+1
[j] −x+1, y−1/2, −z+1
[k] −x+1, y+1/2, −z+1.

3.2. Topological and geometrical structure of the layers

Considering only Ba and As cations, the layers I, II, III and IV are of the same type. All layers show an irregular triangular 3^6 net (Fig. 2). Differences between the four types of layers are attributable to different cation coordination numbers and different orientations of AsO_3OH tetrahedra.

The unit cell includes six layers with a stacking sequence I–II–III–IV–III–II–I (Fig. 1). The layers I and II, II and III, III and IV are shifted relative to each other by approximately $-4a/6$, $b/6$, $c/6$; $-3a/6$, $-b/6$, $c/6$; $-2a/6$, $-b/6$, $c/6$, respectively. The layers are not of a completely equal width due to coordination requirements of the cations and the presence or absence of the screw axis 2_1.

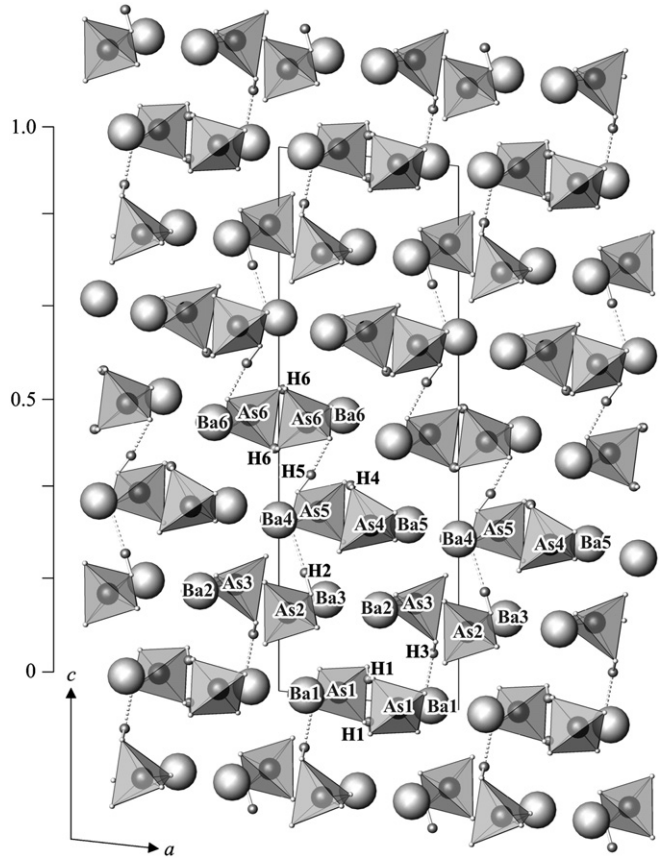

Fig. 1. Crystal structure of $P2_1$-Ba(AsO_3OH) projected along [0 1 0] showing its layered character.

3.3. Cation polyhedra of barium and arsenic

There are six symmetrically independent Ba and six As atoms positioned in the general positions. Ba^{2+} cations show two different types of coordination polyhedra, $BaO_7(OH)_2$ and $BaO_8(OH)_2$. These coordinations are clear-cut, because further oxygen are in the larger distances than As atoms. Of these, Ba1, Ba2, and Ba5 each form ten Ba–O bonds to eight O atoms and two OH groups, while Ba3, Ba4, and Ba6 form nine Ba–O bonds to seven O atoms and two OH groups. The six oxygen atoms located in the same layer and three or four oxygen atoms from the layer above and below are forming the polyhedra vertices. $BaO_7(OH)_2$ and $BaO_8(OH)_2$ polyhedra share trigonal faces ($Ba1O_8(OH)_2$ polyhedra in layer I, $Ba2O_8(OH)_2$ with $Ba3O_7(OH)_2$ in layer II and $Ba4O_7(OH)_2$ with $Ba5O_8(OH)_2$ in layer III) or edges ($Ba6O_8(OH)_2$ polyhedra in layer IV) and build up [0 1 0] zig-zag chains, which sandwich the As atoms.

Average Ba–O lengths are 2.910, 2.922 and 2.934 Å for ten-coordinated Ba1, Ba2 and Ba5, respectively. For nine-coordinated Ba3, Ba4 and Ba6 the average Ba–O lengths are 2.872, 2.862 and 2.874 Å, respectively. This is in agreement with calculated values (2.92 and 2.87 Å) for the sum of effective ionic radii of the Ba^{2+} and O^{2-} ions (1.52 and 1.47 Å for ten- and nine-coordinated Ba^{2+}, respectively [23]). These polyhedra are additionally connected by hydrogen bonds involving all hydroxyl groups.

As–O lengths and O–As–O angles of the $AsO_3(OH)$ tetrahedra are in good agreement with literature values for protonated arsenate tetrahedra: All six As atoms exhibit three short As–O (1.655(5) to 1.689(4) Å) and one long As–O_h length (1.739(5) to 1.772(5)), where O_h is protonated O atom. Whereas the As1–O14, As3–O34 and As6–O64 bond lengths agree well with the average As–O_h value of 36 well-determined AsO_3OH groups (1.731(2) Å [23]), three other As–O_h bond lengths are slightly longer (Table 3).

Each O*x*4 (x=1–6) atom is, besides the corresponding As*x*, additionally bonded to two Ba atoms and is donor of a strong or medium-strong hydrogen bond (Table 3). As a consequence, a relatively long As*x*–O*x*4 bond results. The O–As–O angles are consistent with this interpretation. The largest and smallest angles are associated with the OH groups.

3.4. Hydrogen bonding

The presence of heavy Ba atoms in the structure did not allow the direct location of the H atoms. Nonetheless, there is no ambiguity as to which O atoms they are attached to. On the basis of As–O bond lengths, H atoms can be unambiguously assigned to the oxygen atoms O14, O24, O34, O44, O54 and O64. The hydrogen positions are in agreement with the As–O distances, the longer As–O distances indicating the protonated O atoms in all

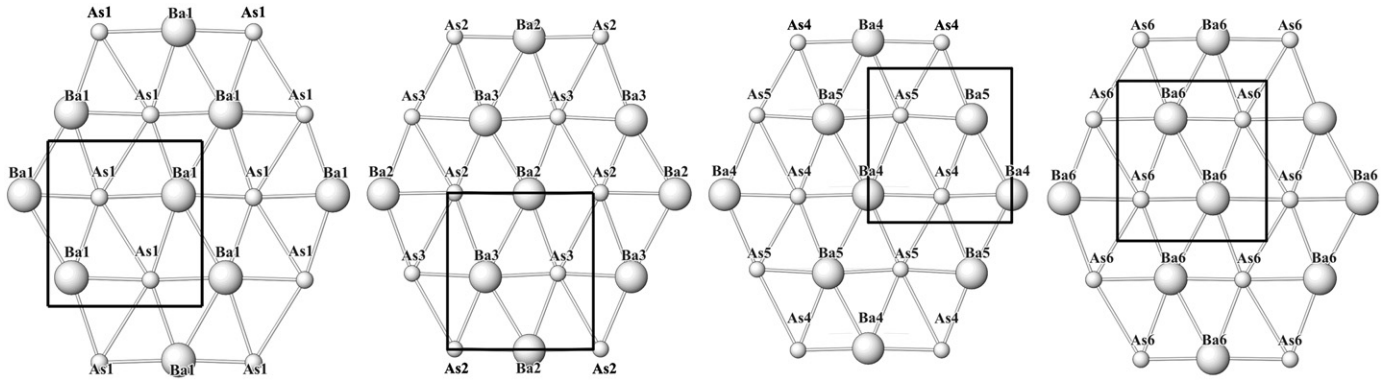

Fig. 2. Mesh type and topological structure of the cation layers seen along [0 0 1]; *a*-axis vertical, *b*-axis horizontal. A trace of the unit cell is drawn for reference.

cases. The bonds donated by O14, O44 and O64 are limited in the 00*z* layers, while those donated by O24, O34 and O54 link adjacent layers.

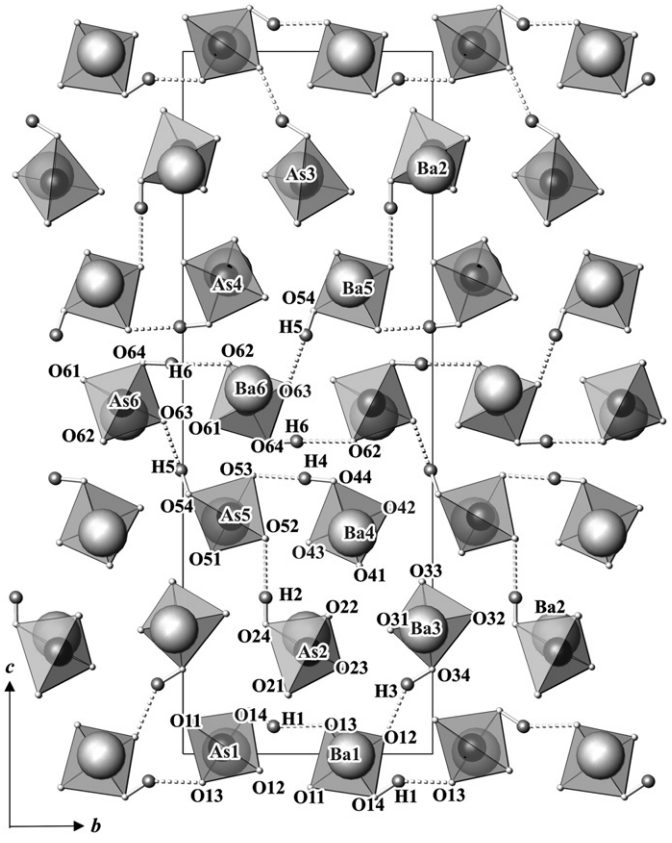

Fig. 3. Projection of the crystal structure of $P2_1$-Ba(AsO_3OH) along [1 0 0]. The hydrogen bonding network and network geometry of the anionic chains are indicated.

Two neighboring $As1O_3(OH)$ tetrahedra are interconnected by very strong hydrogen bonds of 2.462(7) Å (O14H1···O13) in the same, layer I. Additionally, the $As1O_3(OH)$ tetrahedra are connected to $As3O_3(OH)$ by the O34H3···O12 hydrogen bonds of 2.575(7) Å to the next, layer II (Fig. 3). The $As2O_3(OH)$ tetrahedra are linked by a moderately strong hydrogen bond O24–H2···O52 of 2.890(7) Å to $As5O_3(OH)$ in adjacent layer III. The $As4O_3(OH)$ tetrahedra are interconnected by strong hydrogen bond O44–H4···O53 of 2.512(5) Å to $As5O_3(OH)$ in the same layer III. Additionally, the $As5O_3(OH)$ tetrahedra are connected by O54–H5···O63 (=2.623 (6) Å) to the next layer IV. One hydroxyl group, O64H6 from the $As6O_3(OH)$ tetrahedron, act as hydrogen bond donor to O62 from the same layer IV: O64–H6···O62 is 2.644(7) Å.

Two of the AsO_4 tetrahedra are oriented so that two hydrogen bonds (O34–H3···O12 and O14–H1···O13) represent edges in the $Ba1O_8(OH)_2$ and $Ba2O_8(OH)_2$ coordination polyhedra, Therefore H atoms form short Ba···H contacts (2.8864(4), 2.6403(4) Å for Ba1–H3 and Ba2–H1, respectively).

3.5. Bond-valence analysis

The results of bond-valence calculations [25] confirm the presence of divalent barium and pentavalent arsenic. Calculated values range from 1.9 to 2.2 valence units (v.u.) for Σv_{ij}(Ba) and from 4.9 to 5.0 v.u. for Σv_{ij}(As).

The consistency of the hydrogen bonding scheme is tested by calculating bond valences. Taking into account the contribution of non-H atoms only, the O*x*4 (x=1–6) atoms are strongly undersaturated: Σv_{ij}(O*x*4) range from 1.3 to 1.4 v.u. (Table 4). Considering that the O*x*4 atoms are the single donors of very strong to medium-strong hydrogen bonds toward O13, O52, O12, O53, O63 and O62 (for acceptors Σv_{ij}(O) range from 1.7 to 1.8 v.u.), respectively, the bond valences are well balanced. For the remaining O atoms, which are not involved in hydrogen bonding, Σv_{ij}(O) range from 1.9 to 2.1 v.u. The hydrogen bonding geometry is given in Table 3 and Fig. 3 and it is in accordance with the bond valences (Table 4).

Table 4
Bond-valences v_{ij} (valence units) for $P2_1$-Ba(AsO_3OH) (room-temperature data collection). The calculation is based on the parameters given in [25] for the hydrogen bonds according to [34].

	Ba1	Ba2	Ba3	Ba4	Ba5	Ba6	As1	As2	As3	As4	As5	As6	Σv_{ij} [a]	H1	H2	H3	H4	H5	H5	Σv_{ij} [b]
O11	0.22+0.11	–	0.24	–	–	–	1.30	–	–	–	–	–	1.87	–	–	–	–	–	—	1.87
O12	0.30+0.20	–	–	–	–	–	1.30	–	–	–	–	–	1.80	–	–	0.30	–	–	—	2.10
O13	0.22	0.23	–	–	–	–	1.23	–	–	–	–	–	1.68	0.43	–	–	–	—	—	2.11
O14	0.12	0.18	–	–	–	–	1.06	–	–	–	–	–	1.36	0.57	–	–	–	—	—	1.93
O21	0.41+0.07	0.05	–	–	–	–	–	1.35	–	–	–	–	1.88	–	–	–	–	–	—	1.88
O22	–	0.33	–	0.36	–	–	–	1.35	–	–	–	–	2.04	–	–	–	–	—	—	2.04
O23	0.28	0.23	0.26	–	–	–	–	1.28	–	–	–	–	2.05	–	–	–	–	—	—	2.05
O24	–	0.12	0.19	–	–	–	–	0.97	–	–	–	–	1.28	–	0.85	–	–	—	—	2.13
O31	–	0.41	0.36	–	–	–	–	–	1.35	–	–	–	2.12	–	–	–	–	—	—	2.12
O32	–	0.39	0.08	–	0.22	–	–	–	1.33	–	–	–	2.02	–	–	–	–	—	—	2.02
O33	–	–	0.16	0.38	0.15	–	–	–	1.271	–	–	–	1.96	–	–	–	–	—	—	1.96
O34	0.19	–	0.16	–	–	–	–	–	1.06	–	–	–	1.41	–	–	0.70	–	—	—	2.11
O41	–	0.07	0.23	0.30	–	–	–	–	–	1.34	–	–	1.94	–	–	–	–	—	—	1.94
O42	–	–	–	0.16	0.32	0.19	–	–	–	1.30	–	–	1.97	–	–	–	–	—	—	1.97
O43	–	0.20	–	0.20	0.32	–	–	–	–	1.25	–	–	1.97	–	–	–	–	—	—	1.97
O44	–	–	–	0.07	–	0.26	–	–	–	0.99	–	–	1.32	–	–	–	0.64	—	—	1.96
O51	–	–	0.34	–	0.31	–	–	–	–	–	1.35	–	2.00	–	–	–	–	—	—	2.00
O52	–	–	–	0.30	0.21	–	–	–	–	–	1.31	–	1.82	–	0.15	–	–	—	—	1.97
O53	–	–	–	–	0.09	0.34	–	–	–	–	1.23	–	1.66	–	–	–	0.36	—	—	2.02
O54	–	–	–	0.15	0.13	–	–	–	–	–	1.02	–	1.30	–	–	–	–	0.73	—	2.03
O61	–	–	–	–	0.13	0.35+0.11	–	–	–	–	–	1.34	1.93	–	–	–	–	—	—	1.93
O62	–	–	–	0.21	–	0.24	–	–	–	–	–	1.25	1.70	–	–	–	–	—	0.26	1.96
O63	–	–	–	–	–	0.22+0.21	–	–	–	–	–	1.25	1.68	–	–	–	–	0.27	—	1.95
O64	–	–	–	–	0.10	0.08	–	–	–	–	–	1.09	1.27	–	–	–	–	—	0.74	2.01
Σv_{ij}	2.12	2.21	2.02	2.13	1.98	2.00	4.89	4.95	5.01	4.88	4.91	4.93		1.00	1.00	1.00	1.00	1.00	1.00	

[a] Neglecting the contribution from the hydrogen bonds
[b] Including the contribution from the hydrogen bonds.

3.6. Spectroscopic analysis

To obtain further information on the anion groups and especially on hydrogen bonds, polarized single-crystal infrared (4000–400 cm^{-1}) and Raman spectra (4000–60 cm^{-1}) of title compound were acquired (Figs. 4 and 5). Both the IR and the Raman spectra reflect the complexity of the crystal structure. The considerably large numbers of bands below 1000 cm^{-1}, which cannot be unambiguously assigned, are caused by the vibrations of six crystallographically different protonated AsO_4 tetrahedra. Spectroscopic data on protonated orthoarsenates are so far rather incomplete [13,15 and references therein] and not in good agreement with each other. Therefore, attempts to compare with them failed. For comparison purposes, single-crystal infrared spectra of triclinic $F\bar{1}$-Sr(AsO_3OH) and powder infrared spectra and Raman spectra of orthorhombic *Pbca*-Ba(AsO_3OH) were recorded. Their synthesis and crystal structure were published earlier [11]. Comparing the infrared spectra of these three compounds, the distinct frequency ranges may be assigned as follows: in the spectral range between 2900 and 1600 cm^{-1} the presence of vibrational bands that correspond to the OH modes of the $HAsO_4^{2-}$ groups are characterized by three broad bands of the ABC-type in all three compounds (Figs. 4, 6 and 7). These bands are characteristic for strongly hydrogen-bonded crystals. The ABC triplet is a well known phenomenon in the spectroscopy of acid oxy-salts. Claydon and Sheppard [26] showed that the so-called ABC-structure is formed due to the Fermi resonance between the overtones of δOH and γOH and the stretching vibrations *v*OH of the hydrogen bond [27]. Rather than three unrelated bands, the triplet presents a band profile which is commonly believed to result from Fermi resonance interactions between a broad *v*OH stretching band and relatively narrow and weak bands of the 2δOH in-plane and 2γOH out-of-plane bending overtones. In *M*(AsO_3OH) (*M*=Sr, Ba), the ABC-triplet is represented by three intense peaks; in monoclinc $P2_1$-Ba(AsO_3OH) at ca., 2780 (2830), 2337 (2354) and 1700 (1714) cm^{-1}, in triclinic $F\bar{1}$-Sr(AsO_3OH) at ca. 2754 (2772), 2350 (2332) and 1675 (1717) cm^{-1}, respectively, for two different crystal orientations and in orthorhombic *Pbca*-Ba(AsO_3OH) at ca. 2663, 2292 and 1662 cm^{-1}. In the Raman spectra of *Pbca*-Ba(AsO_3OH), ABC triplet is represented with weak broad peaks at ca. 2660, 2272 and 1656 cm^{-1}. The δOH bending vibrations are observed in the region between 1400 and 1110 cm^{-1} in the IR-spectra of all three investigated compounds. The largest difference in the spectra recorded parallel and perpendicular to the crystal

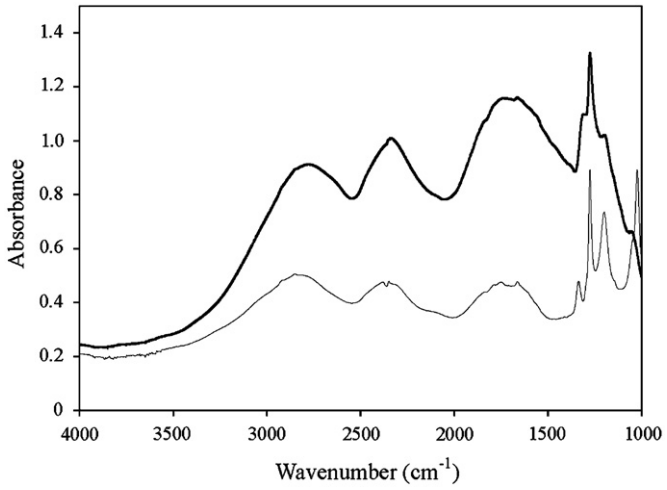

Fig. 4. Single-crystal infrared spectra of $P2_1$-Ba(AsO_3OH) on (bold: parallel to the elongation, thin: perpendicular to the elongation). Bands < 1000 cm^{-1} are truncated due to strong absorption.

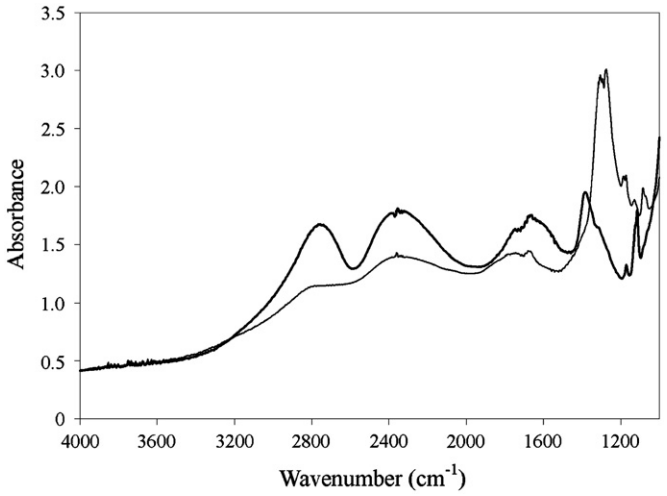

Fig. 6. Single-crystal infrared spectra of $F\bar{1}$-Sr(AsO_3OH) [11] (bold: parallel to the elongation, thin: perpendicular to the elongation). Bands < 1000 cm^{-1} truncated due to strong absorption.

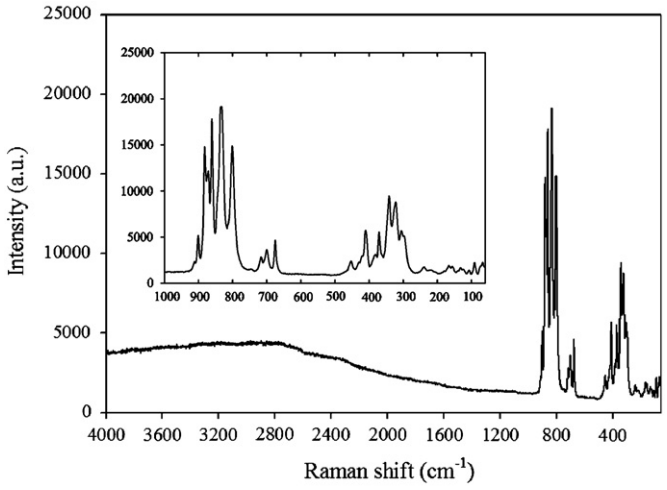

Fig. 5. Raman spectra of $P2_1$-Ba(AsO_3OH).

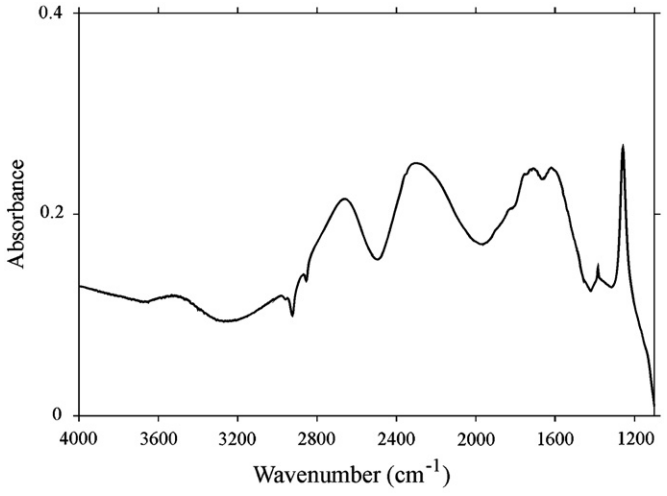

Fig. 7. Powder infrared spectra of *Pbca*-Ba(AsO_3OH) [11].

elongation in this spectral region is the cause of the different orientation of the O–H vectors. Similar bands of ABC-types have been observed in $Ba_2Cu_4(AsO_4)_2(AsO_3OH)_3$ [15].

The wavenumbers of the A or the B bands are in excellent agreement with d–ν correlations for hydrogen bonds given in Ref. [28] and can be related to the strong and medium-strong hydrogen bond lengths of about 2.5–2.8 Å. In the title compound five of six H-bonds are of that type (Table 3). The C band from the triplet may be correlated to the very strong hydrogen bonds of about 2.4–2.5 Å. In $F\bar{1}$-Sr(AsO_3OH) and orthorhombic *Pbca*-Ba(AsO_3OH) the ABC-triplet is in good agreement with O···O bonds (Table 4). Due to the strong absorption, bands below $\sim 1000\ cm^{-1}$ in single-crystal infrared spectra of monoclinic $P2_1$-Ba(AsO_3OH) and triclinic $F\bar{1}$-Sr(AsO_3OH) are truncated and therefore are not further discussed (there was not enough material for the powder IR measurements).

In the 1000–600 cm^{-1} range, Raman spectra (Figs. 5 and 8) of the both polymorphs of $BaAsO_3OH$ show the As–O stretching modes of the $(AsO_3OH)^{2-}$ groups. The number of Raman bands in this region shows the complexity of the crystal structure very well. The intense bands in $P2_1$-$BaAsO_3OH$ the Raman around 882, 875, 872, 861, 834 and 802 cm^{-1} and medium-strong bands around 912, 901, 715, 700 and 676 cm^{-1} correspond to the symmetric and antisymmetric stretching vibrations of $(AsO_3OH)^{2-}$ groups. Similar Raman bands have been observed in $Sr_4Cu_3(AsO_4)_2(AsO_3OH)_4 \cdot 3H_2O$ and $Ba_2Cu_4(AsO_4)_2(AsO_3OH)_3$ [15]. In the powder infrared spectra of the orthorhombic *Pbca*-Ba(AsO_3OH) (Fig. 7) the intense bands around 902, 887, 857 and 821 and medium intense bands around 792 and 728 cm^{-1} correlate well with the Raman bands of the monoclinic $P2_1$-Ba(AsO_3OH). The number of Raman bands in the 1000–600 cm^{-1} range of the orthorombic polymorph (Fig. 8) is smaller as compared to the number of Raman bands of the $P2_1$-Ba(AsO_3OH), but in consistency with the complexity of the two crystal structures. The intense bands around 863, 847 and 789 and medium intense bands around 885, 869 and 727 cm^{-1} correlate well with the Raman bands of the monoclinic $P2_1$-Ba(AsO_3OH).

The modes around 800 ± 20 and $764 \pm 20\ cm^{-1}$ represent antisymmetric stretching modes of the protonated arsenate group. It is known that the $(AsO_4)^{3-}$ group is the only tetrahedral oxyanion of the main group elements in which $\nu_s > \nu_{as}$ [29].

In the region below 550 cm^{-1} appear the bending modes of the $(AsO_3OH)^{2-}$ and $(AsO_4)^{3-}$ groups, and various low-energetic lattice modes of the compound.

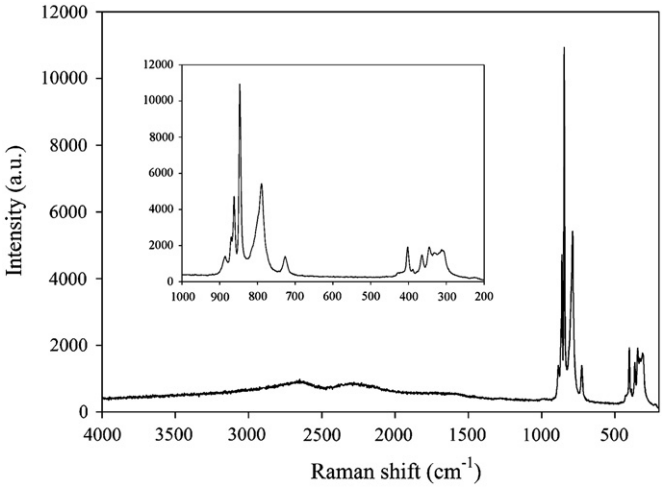

Fig. 8. Raman spectra of *Pbca*-Ba(AsO_3OH) [11].

3.7. Low-temperature structure investigation

Single-crystal data of monoclinic $P2_1$-Ba(AsO_3OH) were collected at low temperature for a further investigation of the hydrogen bonds. As expected the cell volume decreases from room-temperature to 120 K by 7.36‰, as well as the axial angle (1.25‰). The shifts of the atom positions between the room and low temperature refinements are very small, < 0.003, < 0.002 and < 0.004 Å for the Ba, As and O atoms, respectively. The changes of the interatomic distances are at the limit of accuracy of the structure investigations. The average ⟨Ba–O⟩ bonds reduction varies from −2.41‰ to −6.13‰ (see Table 3). Due to the liberation motion of the isolated tetrahedra, the As–O bonds appear shorter as they really are. The shifts of the ⟨As–O⟩ seem to indicate a slight tendency (if realistic) to increase at low temperature. This effect can be estimated considering the oxygen displacement parameters parallel and perpendicular to the As–O bond: ⟨ΔU(par)⟩ values are temperature independent, which is characteristic of AsO_4 rigid-body behavior; ⟨ΔU(perp)⟩, without considering O_h, increases with temperature, which is characteristic of a librational motion of the entire tetrahedron. In addition to the tetrahedral rigid-body libration, the As–O_h vector undergoes an independent librational motion that weakens the O_h–H···O hydrogen bond [30]. This weakening can also be seen in the temperature dependence of the O_h–H···O separation, which increases for the hydrogen bonds from 120 to 293 K (Table 3).

3.8. Relationships to structures of $MHAsO_4$ (M^{2+} = Ca, Sr, Ba) compounds

Crystal structure investigations have shown that hydrogen bonding plays an important role for alkaline earth hydrogen monoarsenates to form anionic networks with different geometries. The network geometries of the above mentioned arsenates consist of different kinds of chains, and chains in the presence of arsenate dimers, the latter being composed of two arsenate tetrahedra connected via very short and short hydrogen bonds (Table 5). Similar to alkaline earth hydrogen phosphates [9] three kind of network geometries are present: simple chains, branched chains and chains in the presence of dimers.

In triclinic $P\bar{1}$-$CaHAsO_4$ [31] there are three topologically distinct hydrogen bonds. One hydrogen atom is located close to an inversion center forming a very short (2.397 Å) symmetry-restricted hydrogen bond O7–H1···O7↔O7···H1–O7. The second hydrogen bond (O1–H2···O5) is an ordered but short (2.582 Å) hydrogen bond, where the donor and acceptor atoms are not related by space-group symmetry. The third hydrogen bond (O6–H3···O8) represents an edge in the $Ca2O_8$ coordination polyhedron. Half of these edges probably represent the third (bent) hydrogen bond where the atom H3 is covalently bonded to the O6 atom; the predominant acceptor is the O8 atom; also a bifurcated bond or a position of the H3 atom at or close to the center of symmetry relating two O6 and two O8 atoms was discussed in Ref. [31]. For triclinic $P\bar{1}$-$SrHAsO_4$ [32] only indexed powder X-ray diffraction data were reported, according to which this compound should be isostructural with the above described $P\bar{1}$-$CaHAsO_4$ [31].

The hydrogen bonding network from $P\bar{1}$-$CaHAsO_4$ is topologically maintained in triclinic $F\bar{1}$-Sr(AsO_3OH) [11]. The superstructure found in $F\bar{1}$-Sr(AsO_3OH) avoids symmetry centers in the H1 and H3 surroundings. All hydrogen atom positions are fully occupied and the hydrogen bonds are ordered. In all eight hydrogen bonds, donor and acceptor atoms are distinct due to the space-group symmetry. Four very short H-bonds (2.466–2.496 Å) and four short H-bonds (2.524–2.616 Å) are present. The network geometry in $P\bar{1}$-$CaHAsO_4$ and in both polymorphs of Sr(AsO_3OH)

Table 5
Selected structural characteristic of some alkaline earth arsenates $M^{II}HAsO_4$ (room-temperature data).

Compound	$CaHAsO_4$	$SrHAsO_4$[a]	$Sr(AsO_3OH)$	$Ba(AsO_3OH)$	$Ba(AsO_3OH)$	$BaHAsO_4$[b]
Reference	[31]	[32]	[11]	[11]	this work	[7]
Space group, Z	$P\bar{1}$, 4	$P\bar{1}$, 4	$F\bar{1}$, 64	*Pbca*, 16	$P2_1$, 12	$P_{orthorhombic}$
a (Å), α (deg.)	7.0591(8), 97.43(2)	7.34(1), 96.0(2)	14.697(3), 95.20(2)	8.581(2), 90	7.2370(2), 90	14.56(2), 90
b (Å), β (deg.)	6.8906(9), 103.55(2)	6.97(1), 103.5(2)	28.230(5), 104.78(3)	9.896(2), 90	7.7133(2), 96.073(2)	19.72(3), 90
c (Å), γ (deg.)	7.2006(16), 87.75(2)	7.40(2), 86.9(2)	14.920(3), 88.11(3)	19.417(4), 90	21.8079(5), 90	4.67(1), 90
V (Å^3)	337.62	365.96	5960.5	1648.8	1210.51(5)	1340.86
D_c (g/cm^3)	3.514	4.133	4.057	4.470	4.564	4.120
Cation radii: $R(M^{II})^{[CN]}$ (Å)[c]	$R(Ca)^{[7]}=1.06$, $R(Ca)^{[8]}=1.12$ $R(Ca1)^{[8]}=1.06$	–	$R(Sr)^{[8]}=1.26$	$R(Ba)^{[9]}=1.47$	$R(Ba)^{[9]}=1.47$, $R(Ba)^{[10]}=1.52$	–
Cation electronegativity	1.0	1.0	1.0	0.9	0.9	0.9
Average distances $\langle M—O\rangle$ (Å)	$\langle Ca1^{[7]}—O\rangle=2.460$ $\langle Ca2^{[8]}—O\rangle=2.496$	–	$\langle Sr1^{[8]}—O\rangle=2.740$ $\langle Sr2^{[8]}—O\rangle=2.710$ $\langle Sr3^{[8]}—O\rangle=2.697$ $\langle Sr4^{[8]}—O\rangle=2.712$ $\langle Sr5^{[8]}—O\rangle=2.623$ $\langle Sr6^{[8]}—O\rangle=2.624$ $\langle Sr7^{[8]}—O\rangle=2.624$ $\langle Sr8^{[8]}—O\rangle=2.626$	$\langle Ba1^{[9]}—O\rangle=2.870$ $\langle Ba2^{[9]}—O\rangle=2.829$	$\langle Ba1^{[10]}—O\rangle=2.910$ $\langle Ba2^{[10]}—O\rangle=2.921$ $\langle Ba3^{[9]}—O\rangle=2.872$ $\langle Ba4^{[9]}—O\rangle=2.862$ $\langle Ba5^{[10]}—O\rangle=2.934$ $\langle Ba6^{[9]}—O\rangle=2.874$	–
Network geometry of anions	Branched chains	Branched chains	Branched chains	Chains (Ch) and Dimers (D)	Branched chains	Simple chains
D···A (Å)	2.397, 2.582, 2.675	–	2.491, 2.496, 2.466, 2.524, 2.616, 2.482, 2.554, 2.584	2.533, 2.533	2.449, 2.883, 2.565, 2.512, 2.617, 2.637	–
As–As (Å)	4.669	–	4.817, 4.551, 4.810	Ch: 4.612, D: 4.483	4.942, 4.491	–
As–As–As (deg.)	149.22	–	149.46, 149.77	136.79	118.34, 114.83,	–
Sample preparation	Pierrot method	Precipitation method	Hydrothermal synthesis at 220 °C	Hydrothermal synthesis at 220 °C	Hydrothermal synthesis at 220 °C	Heating product of $BaHAsO_4\cdot H_2O$
Comment	Isostructural with $CaHPO_4$ [35,36], α-$SrHPO_4$ [37], α-$NaHSO_4$ [38], $HgHPO_4$ [39]		*Super*structure [11]	Isostructural with γ-$SrHPO_4$ [10], $K(SO_3OH)$ [40], $K(SeO_3OH)$ [41]	New structure type	Isostructural with *Pbnm*-$BaHPO_4$ [9]

[a] Only X-ray powder diffraction data were reported and the authors determined the average structure only.
[b] Only X-ray powder diffraction data were reported.
[c] CN: coordination number [23].

is represented by branched chains formed from polar chains of ($As2O_3OH$) groups parallel to [1 0 1], where the ($As1O_3OH$) are branched via the H2 atoms. Neighboring chains point in different directions.

Nabar and Dalvi [7] mentioned orthorhombic $BaHAsO_4$ as a heating product of $BaHAsO_4\cdot H_2O$ and reported only X-ray powder diffraction data. According to them, $BaHAsO_4$ should be isostructural with orthorhombic *Pbnm*-$BaHPO_4$ [9]. The atomic arrangement of *Pbnm*-$BaHPO_4$ consist of linear chains of ($P1O_3OH$) and ($P2O_3OH$) groups parallel to the [1 0 0] and strongly linked by hydrogen bonds. In orthorhombic *Pbca*-$Ba(AsO_3OH)$ [11], short hydrogen bonds are formed between two $As1O_4$ and two $As2O_4$ tetrahedra; however, the linkage is topologically different. Each two $As1O_4$ tetrahedra are linked by two slightly bent hydrogen bonds O4–H1···O1 (2.533 Å) to form a dimer. The $As2O_4$ tetrahedra are linked by practically linear O6–H2···O7 (2.533 Å) hydrogen bonds to infinite chains parallel to [1 0 0]. Neighboring chains point into opposite direction.

The network geometry in the new $P2_1$-$Ba(AsO_3OH)$ is represented by branched chains formed from infinite chains of ($As1O_3OH$) and ($As6O_3OH$) groups parallel to [0 1 0], where the ($As3O_3OH$) are branched via the H3 atoms and ($As2/4/5O_3OH$) are branched via H2/4/5 atoms. The difference between the anionic network geometry of the title compound and chemically similar earth alkali arsenates is in the branching degree that leads to a decrease of the As–As–As angles within the chains. Generally, an increase of As–As distances is accompanied by an increase in the As–As–As angles. The maximum value of the As–As distances is for the straight chains as should be in orthorhombic *Pbnm*-$BaHAsO_4$ [7].

The hydrogen bonds in triclinic $MHXO_4$ and $M(XO_3OH)$ ($M=Na^+$, Ca^{2+}, Sr^{2+}, Hg^{2+}; $X=P^{5+}$, S^{6+}, As^{5+}) compounds were in detailed discussed in Ref. [11].

4. Conclusion

A new polymorph of barium hydrogen arsenate(V) was synthesized using a hydrothermal method. Its crystal structure and vibrational spectra were discussed in detail. It has a layered structure and adopts a new structure type. This work has demonstrated that synthesis of earth alkali arsenates by low-temperature hydrothermal method can still yield novel structure types with interesting crystal-chemical properties, such as very short hydrogen bond lengths, where the donor and acceptor are crystallographically different and ABC-like spectra. The appearance of three $Ba(AsO_3OH)$ polymorphs of different calculated densities might depend on the used synthesis conditions (e.g. temperature, pressure, cooling rate, etc.). Unfortunately, not enough material was available for a possible DTA/TG analyses and further XRD investigations of thermally treated samples.

Further research on the selected metal-arsenates would lead to a detailed understanding on which topologies are expected to form under which conditions (e.g. temperature, pH, ratios of ionic radii…). This information could also be applied to the similar phosphates, vanadates and maybe silicates, which technical use is

based on special physical and chemical behavior that is basically dependent on their crystal structure. Besides potentially interesting properties of arsenates (e.g., ion conductivity, ion exchange and catalytic activities), continuous investigations on their crystal chemistry should be performed because arsenic is known to be one of the most toxic elements in nature. However, arsenates are insufficiently studied, and their crystal-chemical behavior and stability fields are often unknown. Exactly this information is necessary for successful remediation of arsenic in natural systems.

Acknowledgements

Financial support of the Austrian Science Foundation (FWF) (Grant T300-N19) and the Ministry for Science and Technological Development of the Republic of Serbia (Project no. 142030) are gratefully acknowledged. The authors are thankful to Prof. Dr. Eugen Libowitzky for helping with the FTIR and Raman analysis. We appreciate the useful comments of the anonymous reviewers, which helped to improve the text of the manuscript.

Appendix A. Supporting information

Supplementary data associated with this article can be found in the online version at doi:10.1016/j.jssc.2010.09.027.

References

[1] S.B. Hendricks, J. Phys. Chem. 30 (1926) 248–253.
[2] H. Guerin, Compt. Rend. 206 (1938) 1300–1303.
[3] V.J. Iyer, M.A. Nabar, Naturwissenschaften 51 (1964) 240–241.
[4] R.G. Robins, Metall. Trans. 16B (1985) 404–406.
[5] C. Martin, A. Durif, M.T. Averbuch-Pouchot, Bull. Soc. Fr. Minéral. Cristallogr. 93 (1970) 397–398 in French.
[6] D. Blum, A. Durif, J.C. Guitel, Acta Crystallogr. B33 (1977) 3222–3224 in French.
[7] M.A. Nabar, A.P. Dalvi, Monatsh. Chem. 109 (1978) 673–679 in German.
[8] G. Burley, J. Res. Natl. Bur. Stand. A. Phys. Chem. 60 (1958)) 23.
[9] T. Ben Chaabane, L. Smiri, A. Bulou, Solid State Sci. 6 (2004) 197–204.
[10] L. Ben Taher, L. Smiri, Y. Laligant, V. Maisonneuve, J. Solid State Chem. 152 (2000) 428–434.
[11] T. Mihajlović, H. Effenberger, Z. Kristallogr. 221 (2006) 770–781.
[12] T. Mihajlović, H. Effenberger, Mineral. Mag. 68 (2004) 757–767.
[13] T. Mihajlović, E. Libowitzky, H. Effenberger, J. Solid State Chem. 177 (2004) 3963–3970.
[14] T. Mihajlović, U. Kolitsch, H. Effenberger, J. Alloys Compd. 379 (2004) 103–109.
[15] T. Đorđević, Lj. Karanović, J. Solid State Chem. 181 (2008) 2889–2898.
[16] M. Weil, T. Đorđević, C.L. Lengauer, U. Kolitsch, Solid State Sci. 11 (2009) 2111–2117.
[17] Z. Otwinowski, W. Minor, Meth. Enzymol 276 (1997)) 307.
[18] Z. Otwinowski, D. Borek, W. Majewski, W. Minor, Acta Crystallogr. A59 (2003) 228.
[19] G.M. Sheldrick, SHELXS-97, A Program for the Solution of Crystal Structures, University of Göttingen, Germany, 1997.
[20] G.M. Sheldrick, SHELXL-97, A Program for Crystal Structure Refinement, University of Göttingen, Germany, 1997.
[21] M. Nardelli, J. Appl. Crystallogr. 32 (1999) 563–571.
[22] E. Dowty, ATOMS 6.1, a computer program, Kingsport, TN, 1999.
[23] R.D. Shannon, Acta Crystallogr. A32 (1976) 751–767.
[25] N.E. Brese, M. O'Keeffe, Acta Crystallogr. B47 (1991) 192–197.
[26] M.F. Claydon, N. Sheppard, Chem. Commun. 23D (1969) 1431–1433.
[27] S. Bratos, L. Lascombe, A. Novak, OH stretching band of hydrogen-bonded systems in condensed phases, in: H. Ratajczak, W.J. Orville-Thomas (Eds.), Molecular Interactions, Wiley, Chichester, 1980.
[28] E. Libowitzky, Mh. Chem. 130 (1999) 1047–1059.
[29] A.G. Nord, P. Kierkegaard, T. Stefanidis, J. Baran, Chem. Commun. 5 (1988) 1–40 University Stockholm.
[30] D. Nyfeler, C. Hoffmann, T. Armbruster, M. Kunz, E. Libowitzky, Am. Mineral. 82 (1997) 841–848.
[31] G. Ferraris, G. Chiari, Acta Crystallogr. B26 (1970) 403–410.
[32] M.A. Nabar, A.P. Dalvi, Bull. Soc. Fr. Minéral. Cristallogr 100 (1977) 353–354.
[33] R.X. Fischer, E. Tillmanns, Acta Crystallogr. C44 (1988) 775–776.
[34] G. Ferraris, G. Ivaldi, Acta Crystallogr. B44 (1988) 341–344.
[35] M. Catti, G. Ferraris, A. Filhol, Acta Crystallogr. B33 (1977) 1223–1229.
[36] M. Catti, G. Ferraris, S.A. Mason, Acta Crystallogr. B36 (1980) 254–259.
[37] A. Boudjada, R. Masse, C.J. Guitel, Acta Crystallogr. B34 (1978) 2692–2695.
[38] C. Werner, S.I. Troyanov, H. Worzala, E. Kemnitz, Z. Anorg. Allgem. Chem. 622 (1996) 337–342 in German.
[39] E. Dubler, L. Beck, L. Linowsky, G.B. Jameson, Acta Crystallogr. B37 (1981) 2214–2217.
[40] F. Payan, R. Haser, Acta Crystallogr. B32 (1976) 1875–1879.
[41] J. Baran, J.T. Lis, Acta Crystallogr. C42 (1986) 270–272.